High-Efficiency Coupling-Insensitive Transcutaneous Power and Data Transmission Via an Inductive Link

CLEMENS M. ZIERHOFER AND ERWIN S. HOCHMAIR

Abstract—**This paper presents a new approach for transmitting RF power and signal via an inductive link. Such an approach optimizes the power efficiency of the overall transmission scheme comprising the power amplifier plus the inductive link. Power amplification is based on the single ended class E concept. The power amplification stage is self oscillating, the oscillation frequency thus being influenced by the coupling of the coils. The resulting operating frequency offset yields an improved power transmission performance of the circuit since the oscillation frequency tracks the absolute transmission efficiency maximum. A detailed analysis is given. Realization of the described approach requires a minimal number of circuit components. Experimental and theoretical results are in good agreement.**

I. Introduction

ONE POSSIBILITY for providing an implanted stimulator transcutaneously with power and/or information is to transmit RF power via an inductive link. An inductive link generally consists of two resonant circuits, one external and the other as part of an implanted stimulator. The inductivities of the two resonant circuits are realized by two pancake shaped coils. When facing each other, they form a transformer which allows energy transfer from the transmitter to the implant. Inductive links have been investigated with regard to optimization of efficiency of the power transfer and the tolerance to coupling coil misalignment [1]–[5]. All these links are designed to operate at a fixed operating frequency.

The transfer resonant circuit is either series- or parallel tuned. A series-tuned transmitter requires a voltage source, whereas a parallel tuned transmitter is driven by a current source. A voltage source can be realized with two transistor switches which simply switch the input of the series tuned transmitter between the rails of the power supply (i.e., a class D amplifier, e.g., used in [2] and [6]). A single transistor can act as a current source, capable of driving a parallel tuned transmitter circuit (e.g., class C amplifier). In both cases radio frequency has to be generated by an RF oscillator.

Overall efficiency of a power transmission scheme is defined as the ratio of power delivered to the load (implant) and the overall dc power consumed by the whole system. The overall efficiency of a transmission scheme consisting of RF oscillator, power amplifier, and inductive link including load is determined by the power consumption of the RF oscillator, the efficiency of the power amplifier, and the efficiency of the inductive link itself. Earlier designs were aimed at optimizing exclusively the performance of the inductive link. This paper presents an approach for optimizing the whole transmission scheme in terms of the two criteria, overall efficiency and tolerance to coil misalignment.

Overall efficiency and tolerance to coil distance variations exert a mutual influence on one another. The electronic circuits of most implants require a sufficiently stable voltage supply to ensure optimum operation. If the transmitted RF energy is highly dependent on the mutual coil position, efficiency is noticeably reduced by power losses due to voltage regulators within the implant, which are necessary for the provision of an adequate supply voltage.

The approach used here for the realization of a coupling-insensitive high efficiency power/data link is based on the high efficiency class E power amplification concept. The idea was to combine a class E amplifier with a tuned inductive link. In addition, the class E amplifier is self oscillating. Oscillation frequency is not fixed, but influenced by the mutual position of the coils. This self oscillating final stage has two basic advantages over a driven RF amplifier. First, no oscillator is necessary for generating an RF voltage, thus avoiding additional power losses. Second, oscillation frequency offset due to coupling variations significantly improves power transmission performance since the resulting oscillation frequency tracks the absolute transmission efficiency maximum, whose spectral location is dependent on the coil coupling [see Section III-A.2].

II. Class E Tuned Power Oscillator Involving an Inductive Link

The fundamentals of the class E power amplification concept have been broadly discussed in the literature [7]–[10] and application examples have been presented [11], [12]. An example of the combination of a class E tuned power oscillator and an inductive link is depicted in Fig. 1.

In this case the series tuned output circuit of an ordinary class E power amplifier is replaced by a stagger tuned inductive link. The inductive link is represented by a parallel resonant receiver circuit (L_2, C_2, R_2) which is cou-

Manuscript received February 17, 1989; revised October 23, 1989.
The authors are with the Inst. of Experimentalphysik, Angewandle Physik, Universitaet Innsbruck, A-6020 Innsbruck, Austria.
IEEE Log Number 9035444.

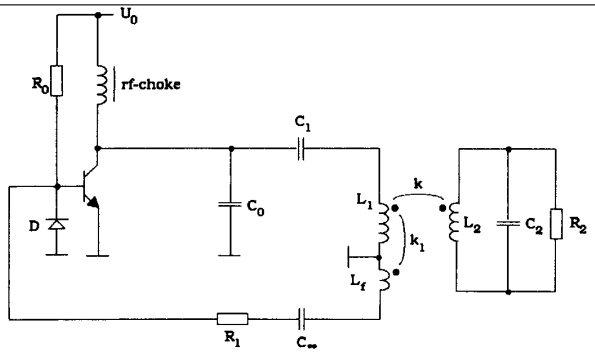

diode D: HP2 800 429
transistor: 2 N 2369 A
rf-choke: 1 mH
R_0: 20 kΩ
C_∞: 100 nF
other specifications see table 1

Fig. 1. Class E tuned power oscillator including an inductive link.

pled to a series tuned transmitter (L_1, C_1). Oscillation is achieved by means of a feedback branch (L_f, C_∞, R_1). Diode D and resistor R_0 provide proper bias voltage and ensure easy starting of oscillation.

The class E concept efficiently permits conversion of dc-battery power to ac power at the switching frequency. A class E amplifier contains a single transistor, which is assumed to operate as a switch, i.e., collector-emitter voltage is essentially zero with nonzero collector current, and vice versa, collector current is about zero when collector-emitter voltage is applied. One basic condition for high efficiency operation is that the switch turn-on resistance of the transistor (i.e., collector-emitter saturation resistance R_{sat}) be comparatively small compared to the ohmic part R of the input impedance $Z_{in} = R + jX$ of the class E output circuit. In contrast to an ordinary class E amplifier where resistance R is equal to the load, R in the present application is dependent on operating frequency f_0 and on the coupling factor k, i.e., $R = R(f_0, k)$. In the case of comparatively weak coupling of the coils (i.e., $0.1 < k < 0.3$), R_{sat} is not negligible in comparison to $R(f_0, k)$ in the analysis.

III. Analysis

A. Frequency Analysis

To analyze the properties of the oscillator depicted in Fig. 1, the circuit is cut at the feedback branch and, in making investigations, it is assumed to be driven by an external frequency source (frequency analysis). An equivalent circuit is shown in Fig. 2.

This is based on the following assumptions:

- the RF choke allows only a constant (dc) input current I_0 and has no series resistance;
- the switching transistor can be described as an ideal switch in series with an ohmic resistor R_{sat};
- the total shunt capacitance C_0 is independent of the collector-emitter voltage;
- resistor R_f consists of resistor R_1 plus an additional loss $\bar{R}$. $\bar{R}$ represents the ohmic resistance due to diode D, resistor R_0 and the base-emitter input resistor of the transistor switch. It is averaged over one time period.

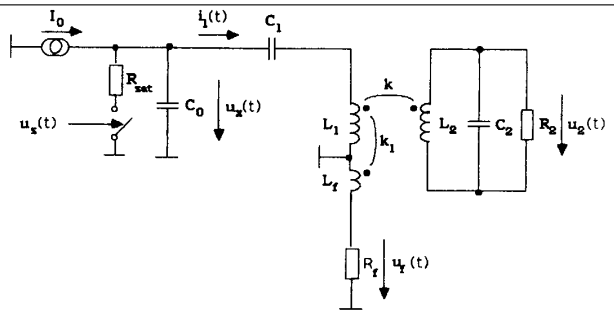

Fig. 2. Equivalent circuit for frequency analysis.

Frequency analysis can be considered in two parts, i.e., into class E analysis and link analysis.

1) Class E Analysis: The analysis of the class E amplifier is performed using the above listed assumptions. The inductive link together with the feedback network is represented by the complex input impedance Z_{in}. In the following, the real and imaginary parts are designated as R and X, i.e., $Z_{in} = R + jX$.

It is assumed that the series reactance X applies to the fundamental frequency only and is infinite at harmonic frequencies. This allows the statement

$$i_1(t) = i_0 \sin(\omega t - \varphi) \tag{1}$$

with amplitude i_0 and phase φ to be determined. A time period T is divided into two equal sections, (i.e., the duty ratio is 50%), the transistor being switched off during the first section, and on during the second. Collector-emitter voltage $u_x(t)$ within the switch-off-state ($0 < t < T/2$) then is

$$u_{x\text{off}}(t) = U_{xo} + \frac{1}{C_0}\int_0^t I_0 - i_1(t)\,dt$$

$$= U_{xo} + \frac{1}{\omega C_0}\left[I_0\omega t + i_0\cos(\omega t - \varphi) - \cos\varphi\right] \tag{2}$$

with U_{xo} as collector voltage at times $t = \cdots -2t, -T, 0, T, 2T, \cdots$.

Determination of $u_x(t)$ in switch-on-state ($T/2 < t < T$) may be achieved by means of Laplace transformation. The result is

$$u_{x\text{on}}(t) = I_0 R_{sat} - \frac{i_0 R_{sat}}{1 + (\omega\tau)^2}\left[\sin(\omega t - \varphi) - \omega\tau\cos(\omega t - \varphi)\right] + \left[U_{x1} - I_0 R_{sat} + \frac{i_0 R_{sat}}{1 + (\omega\tau)^2} \cdot (\sin\varphi + \omega\tau\cos\varphi)\right]\exp\left(\frac{\pi - \omega t}{\omega\tau}\right) \tag{3}$$

with U_{x1} as collector voltage at times $t = \cdots 3T/2, -T/2, T/2, 3T/3, \cdots$, and $\tau = R_{sat} \cdot C_0$. The third term of the sum describes the exponential discharging of capacitor C_0, when the switch is turned on.

Assuming $(\omega\tau)^2 << 1$ yields

$$\tan\varphi = \frac{\left(1 + \frac{\pi}{2}\omega\tau\right)R + \frac{\pi}{2}X + \left(\frac{2}{\pi} - \frac{\pi}{4} + \frac{\omega\tau}{2}\right)\frac{1}{\omega C_0}}{-\left(1 + \frac{\pi}{2}\omega\tau\right)X + \frac{\pi}{2}R + \left(\frac{1}{2} + \omega\tau\left(\frac{\pi}{2} + \frac{2}{\pi}\right)\right)\frac{1}{\omega C_0}} \tag{9}$$

and

$$\frac{i_0}{I_0} = \frac{1}{\left(\omega C_0 X - \frac{1}{2} - \frac{2}{\pi}\omega\tau\right)\sin\varphi + \left(\omega C_0 R + \frac{2}{\pi} + \frac{1}{2}\omega\tau\right)\cos\varphi}. \tag{10}$$

$$U_{xo} = u_{xon}(t = T) \approx I_0 R_{sat} + i_0 R_{sat}(\sin\varphi + \omega\tau\cos\varphi)$$

$$U_{x1} = u_{xoff}(t = T/2) = U_{xo} + (I_0\pi - 2i_0\cos\varphi)/(\omega C_0). \tag{4}$$

Now collector-emitter voltage $u_x(t)$ can be completely determined for both halves of the period

$$u_{xoff}(t) = \frac{1}{\omega C_0}\left[I_0\omega(t + \tau) + i_0[\omega\tau\sin\varphi - \cos\varphi + \cos(\omega t - \varphi)]\right]$$

$$u_{xon}(t) = \frac{1}{\omega C_0}\left[I_0\omega\tau - i_0\omega\tau\sin(\omega t - \varphi) + i_0(\omega\tau)^2\cos(\omega t - \varphi) + [\pi I_0 + 2i_0\omega\tau\sin\varphi - 2i_0\cos\varphi] \cdot \exp\frac{\pi - \omega\tau}{\omega t}\right]. \tag{5}$$

Amplitude i_0 and phase φ are determined as follows: a sinusoidal current $i_1(t)$ would cause a sinusoidal voltage $u_x'(t)$ over impedance $Z_{in} = R + jX$;

$$u_x'(t) = i_0 R\sin(\omega t - \varphi) + i_0 X\cos(\omega t - \varphi). \tag{6}$$

This fictitious voltage must be equal to the component of the Fourier series of the actual collector voltage $u_x(t)$ at the fundamental frequency. The complex Fourier coefficient c_1 is obtained with

$$c_1 = \frac{1}{T}\int_0^T u_x(t)\exp(-j\omega t)\,dt = \frac{1}{T}\left[\int_0^{T/2} u_{xoff}(t)\exp(-j\omega t)\,dt + \int_{T/2}^T u_{xon}(t)\exp(-j\omega t)\,dt\right] \tag{7}$$

The corresponding coefficient c_1' of $u_x'(t)$ is

$$c_1' = \frac{1}{T}\int_0^T u_x'(t)\exp(-j\omega t)\,dt. \tag{8}$$

Setting $c_1 = c_1'$ yields, after comparison of real and imaginary parts, two equations containing i_0 and φ. Solving for i_0 and φ gives

For the special case $R_{sat} = 0$, these results agree with the corresponding results found in [9]. The supply voltage U_0 is equal to the dc component of $u_x(t)$. Using

$$U_0 = \frac{1}{T}\int_0^T u_x(t)\,dt \tag{11}$$

and i_0/I_0 from above, dc-resistance $R_{dc} = U_0/I_0$ can be estimated:

$$R_{dc} = \frac{1}{\omega C_0}\left[\left(\frac{\pi}{4} + \frac{3}{2}\omega\tau\right) + \frac{i_0}{I_0}\left(\left(\frac{\omega\tau}{2} + \frac{1}{\pi}\right) \cdot \sin\varphi - \frac{1}{2}\cos\varphi\right)\right]. \tag{12}$$

Efficiency of this idealized class E scheme is determined by two effects, i.e., by the power consumption of resistor R_{sat} in the on-state and by collector-emitter voltage $u_x(t)$ across capacitor C_0 at times $\cdots -3T/2, -T/2, T/2, 3T/2 \cdots$ (i.e., U_{x1}). The second loss mechanism can be minimized by proper circuit design.

2) Link Analysis: Link analysis is achieved with the help of Fig. 3. It depicts an equivalent circuit of the inductive link including the feedback branch.

To determine the overall two port describing the inductive link, two port A (index a) containing all coupled coils first is evaluated. It is assumed that coil L_f is just coupled to coil L_1 (coupling factor k_1), but not to coil L_2. Then impedance matrix Z_{aik} becomes

$$Z_{aik} = \begin{bmatrix} Z_{a11} & Z_{a12} \\ Z_{a21} & Z_{a22} \end{bmatrix} = \begin{bmatrix} j\omega L_1 + \omega^2 k_1^2 \frac{L_1 L_f}{R_f + j\omega L_f} & j\omega k\sqrt{L_1 L_2} \\ j\omega k\sqrt{L_1 L_2} & j\omega L_2 \end{bmatrix}. \tag{13}$$

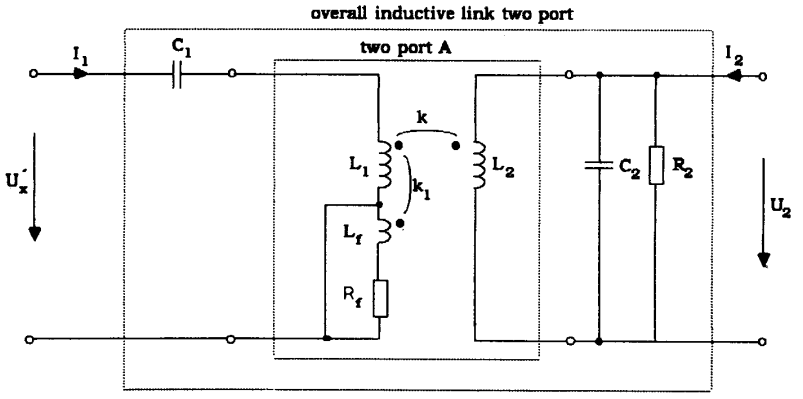

Fig. 3. Inductive link.

This matrix is transformed into the hybrid matrix H_{aik} with relation

$$H_{aik} = \begin{bmatrix} H_{a11} & H_{a12} \\ H_{a21} & H_{a22} \end{bmatrix} = \frac{1}{Z_{a22}} \begin{bmatrix} \det Z_{aik} & Z_{a12} \\ -Z_{a21} & 1 \end{bmatrix}. \quad (14)$$

The hybrid matrix H_{ik} of the overall two port now can be simply obtained as

$$H_{ik} = \begin{bmatrix} H_{11} & H_{12} \\ H_{21} & H_{22} \end{bmatrix} = \begin{bmatrix} H_{a11} + \dfrac{1}{j\omega C_1} & H_{a12} \\ H_{a21} & \left(H_{a12} + j\omega C_2 + \dfrac{1}{R_2} \right) \end{bmatrix}. \quad (15)$$

Using equations

$$U_x' = H_{11} I_1 + H_{12} U_2$$
$$I_2 = H_{21} I_1 + H_{22} U_2 = 0 \quad (16)$$

(complex pointers I_1, I_2, U_x', U_2 referring to Fig. 3) yields the input impedance Z_{in} of the inductive link:

$$Z_{in} = \det (H_{ik}) / H_{22}. \quad (17)$$

Inserting $Z_{in} = R + jX$ into (9) and (10) now fully defines the class E amplifier and consequently the complete system. Output voltage U_2 and overall efficiency η are calculated with matrix H_{ik} and (10) and (12):

$$U_2 = -\frac{H_{21}}{H_{22}} i_0 = -\frac{H_{21}}{H_{22}} \frac{i_0}{I_0} \frac{U_0}{R_{dc}} \quad (18)$$

and

$$\eta = \frac{|U_2|^2}{2R_2 U_0 I_0} = \frac{1}{2R_2} \left| \frac{H_{21}}{H_{22}} \right|^2 \left(\frac{i_0}{I_0} \right)^2 \frac{1}{R_{dc}}. \quad (19)$$

Function $\eta(f)$ is plotted in Fig. 4 for various coupling factors. The calculation is based on circuit specifications

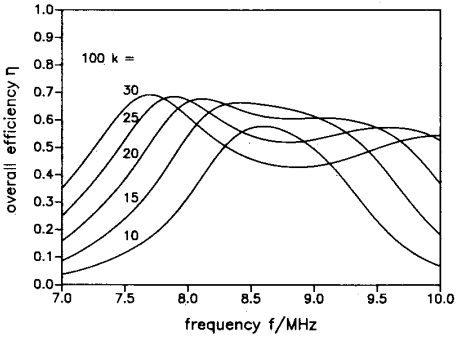

Fig. 4. Calculated overall efficiency $\eta(f)$ for various couplings.

TABLE I
CIRCUIT SPECIFICATIONS

U_0	3.5	V
L_1	2.35	
L_2	3.4	μH
L_f	0.42	
k_1	0.36	
C_0	213	
C_1	217	pF
C_2	101	
R_2	1500	
R_f	200	Ω
R_{sat}	8	

summarized in Table I. These values are also used for the following plots.

Fig. 4 shows that, for a given coupling, the absolute maximum efficiency is achieved in a frequency region between 7.5–8.5 MHz. Within this region, efficiency peaks move towards higher frequencies with decreasing coupling factor k.

B. Oscillator Analysis

Oscillation frequency f_o of the class E oscillator is characterized by the fact that the phase shift between switch

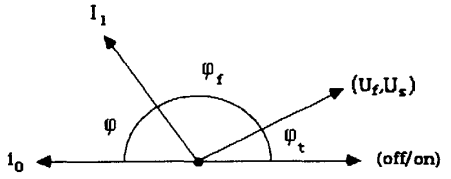

Fig. 5. Basic phase diagram.

voltage U_s and feedback voltage U_f is zero (compare Fig. 2). Fig. 5 defines the phase relations of the circuit signals used to determine the oscillation frequency.

The pointer (off/on) indicates the actual switching phase of the transistor switch versus pointer i_0. The phase shift of π between these pointers is due to the initial definition of $i_1(t)$ [compare (1)]. The phase shift φ_t between pointers (off/on) and pointer (U_f, U_s) represents a switching delay of the transistor versus base-emitter voltage U_f, i.e., U_s (within the closed feedback configuration feedback voltage U_f is identical to switching voltage U_s). This is due to dynamic effects within the transistor at high frequencies. Phase shift φ_f can be estimated with the help of hybrid matrix H_{ik}. The result is

$$\varphi_f = \pi - \text{arc } tg \frac{R_f}{\omega L_f}. \tag{20}$$

Note, that both phase shifts φ_t and φ_f are independent of the coupling factor k.

Phase shift $\varphi(f)$ between pointers i_0 and I_1 is determined by (9). It is depicted in Fig. 6 as a function of operating frequency f for various coupling factors k.
All curves $\varphi(f)$ intersect at point S. At this point, phase shift $\varphi(f)$ is independent of coupling factor k.

It can easily be proved that, given that two curves $\varphi(f)$ with different coupling intersect, then all curves do so: with the help of (15) and (17), (9) can always be reduced to a general form

$$tg\varphi = \frac{a(f) + k^2 b(f)}{c(f) + k^2 d(f)} \tag{21}$$

with $a(f)$, $b(f)$, $c(f)$, and $d(f)$ as real polynomial functions of frequency f. Phase shift $\varphi(f)$ is independent of coupling k if and only if

$$\frac{a(f)}{b(f)} = \frac{c(f)}{d(f)}. \tag{22}$$

Each real solution of this algebraic equation defines an intersection point of all curves $\varphi(f)$ for arbitrary coupling factors k.

Oscillation frequency f_o is determined by the following relation

$$\pi - \varphi_t - \varphi_f = \varphi. \tag{23}$$

The left side of this equation is independent of coupling factor k and comparatively weakly dependent on frequency f. In a first approximation it can be assumed to be

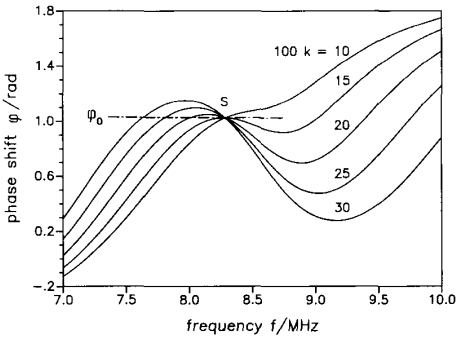

Fig. 6. Calculated phase shift $\varphi(f)$ for various couplings.

constant within the operating frequency range, i.e.,

$$\pi - \varphi_t - \varphi_f \approx \varphi_0 = \text{constant}. \tag{24}$$

Operating points are defined by the intersection points of the straight line φ_0 and curves $\varphi(f)$. In this connection, intersection point S plays an important role. Experimental and theoretic investigations show that the performance of the circuit in terms of overall efficiency and insensitivity of output voltage U_2 to coupling variations are optimized, if the straight line φ_0 defined above contains intersection point S.

If coupling is sufficiently high (compare Fig. 6, curves with $k = 0.3, 0.25, 0.2, 0.15$), there exist three intersection points of phase $\varphi(f)$ with the straight line φ_0. In this case point S is not a stable operating point since

$$\frac{\delta\varphi(f)}{\delta f} < 0. \tag{25}$$

Two stable operating points, i.e., two possible oscillation frequencies for each solution, remain. If coupling drops below a certain limit, the only stable operating point is point S (compare curve $\varphi(f)$ *for* $k = 0.1$ of Fig. 6).

Which of the two stable operating points is preferred by the system is explained assuming that the coupling of the coils is being slowly increased. At low coupling the only stable operating point is S, as explained above. The coupling is now increased until the condition

$$\frac{\delta\varphi(f)}{\delta f} = 0 \tag{26}$$

is reached in point S. S is still the only stable operation point. Any further increase of k forces the system to decide between two intersection points left or right of S. S itself is not stable, since (25) is valid. Theoretically neither right nor left is preferred; the probability is 0.5 for both cases. This decision can be avoided, if S does not lie on straight line φ_0. E.g., if S is somewhat below φ_0, the operating points of the system will be left of S at increasing coupling. In every intersection point left of S condition

$$\frac{\delta\varphi(f)}{\delta f} > 0 \tag{27}$$

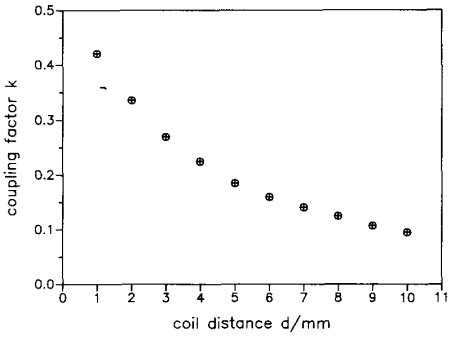

Fig. 7. Measured coupling factor k as a function of spatial coil distance d.

is valid. If S is above φ_0, the system will prefer operation points right of S. Thus in practical applications a left/right preference of the circuit operating points can be achieved by proper adjustment of φ_0.

The operating points situated to the left of point S move towards higher frequencies, if coupling factor k is decreased. A comparison with Fig. 4 shows that these operating points are tracking the absolute maximums of the overall efficiency. The behavior of the output voltage U_2 in terms of coupling variations is treated below. In the following, calculation and experimental results are compared. Fig. 7 depicts coupling factor k measured as a function of spatial coil distance d.

Fig. 8 plots the following functions

- oscillation frequency f_0
- overall efficiency η and
- output voltage U_2,

calculated and measured as a function of spatial coil distance d. Calculation is based on circuit specification of Table I and relationship $k(d)$ of Fig. 7. The feedback phase is determined by the location of point S. Calculation yields $\varphi_0/\text{rad} = 1.0278$.

Output voltage U_2 is almost independent of coupling up to a coil distance $d = 8$ mm. Within this range overall efficiency varies between 60 and 70%.

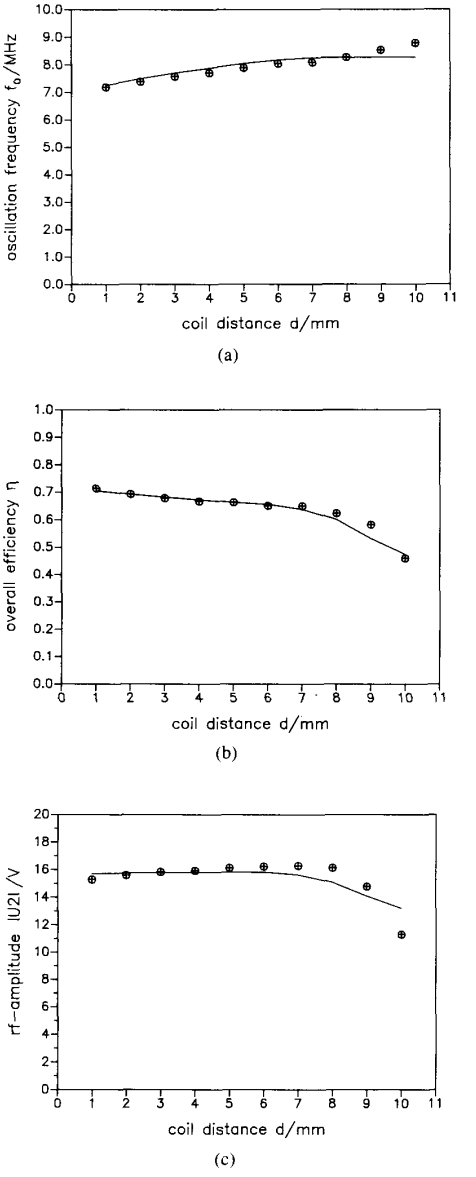

Fig. 8. (a) Oscillation frequency f_0. (b) Overall efficiency η. (c) Output voltage U_2. ⊕ indicates experimental results.

IV. Data Transmission

In principle the system described can be used for inductive transmission of information. Practical schemes are

- amplitude modulation (AM) to convey an analog waveform, or
- amplitude shift keying (ASK) to transmit digital data.

AM and ASK can be achieved to modulation of supply voltage U_0 of the transmitter circuit. A more detailed description of the AM and ASK performance of the circuit will be presented in a forthcoming paper.

V. Conclusion

The feature of the system described in the present paper may be summarized as follows:

1) A high overall efficiency is obtained, even if coil coupling is comparatively low. Thus heavy ferrite backings of the coils used in some applications to improve coil coupling [2] may be avoidable.

2) The RF voltage amplitude is extremely insensitive to coupling variations within a wide coupling range.

3) For realization of the transmission scheme a minimal number of circuit components is necessary. The only active element is a single transistor switch.

4) The operating frequency is not fixed, but influenced by the coil coupling.

5) Referring to point 4), a practical scheme for transmitting power and digital data, is e.g., amplitude shift keying.

REFERENCES

[1] J. C. Shuder, H. E. Stephenson, and J. F. Townsend, "High-level electromagnetic energy transfer through a closed chest wall," in *IRE Int. Conv. Rec.*, part. 9, vol. 9, pp. 119-126, 1961.

[2] D. C. Galbraith, M. Soma, and R. L. White, "A wide-band efficient inductive transdermal power and data link with coupling insensitive gain," *IEEE Trans. Biomed. Eng.*, vol. BME-34, pp. 265-275, Apr. 1987.

[3] J. Steurer and E. Hochmair, "Transcutane signal-und leistungsübertragung für implantate über hochfrequenz-bandfilter," *Biomed. Tech.*, Band 31, Heft 4, 1986.

[4] E. S. Hochmair, "System optimization for improved accuracy in transcutaneous signal and power transmission," *IEEE Trans. Biomed. Eng.*, vol. BME-31, pp. 177-186, Feb. 1984.

[5] W. H. Ko, S. P. Liang, and C. D. F. Fung, "Design of radio-frequency powered coils for implant instruments," *Med. Biol. Eng. Comput.*, vol. 15, pp. 634-640.

[6] N. de N. Donaldson, and T. A. Perkins, "Analysis of resonant coupled coils in the design of radio-frequency transcutaneous links," *Med. Biol. Eng. Comput.*, vol. 21, pp. 612-627, 1983.

[7] N. O. Sokal and A. D. Sokal, "Class E, a new class of high-efficiency tuned single-ended switching power amplifiers," *IEEE J. Solid-State Circuits*, vol. SC-10, no. 3, pp. 168-176, June 1975.

[8] N. O. Sokal, "Class E high-efficiency switching-mode tuned power amplifier with only one inductor and one capacitor in load network-approximate analysis," *IEEE J. Solid-State Circuits*, vol. SC-16, no. 4, Aug. 1981.

[9] F. H. Raab, "Idealized operation of the class E tuned power amplifier," *IEEE Trans. Circuits Syst.*, vol. CAS-24, pp. 725-735, Dec. 1977.

[10] ——, "Effects of circuit variations on the class E tuned power amplifier," *IEEE J. Solid-State Circuits*, vol. SC-13, pp. 239-247, Apr. 1978.

[11] J. Ebert and M. Kazimierczuk, "Class E high efficiency tuned power oscillator," *IEEE J. Solid-State Circuits*, vol. SC-16, pp. 62-66, Apr. 1981.

[12] M. Kazimierczuk, "Collector amplitude modulation of the class E tuned power amplifier," *IEEE Trans. Circuits Syst.*, vol. CAS-31, vol. 6, pp. 543-549, June 1984.

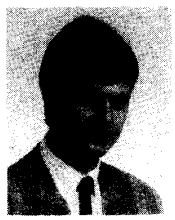

Clemens M. Zierhofer was born in Innsbruck, Austria, in 1962. He received the Dipl. Ing. and Dr.techn. degrees in electrical engineering from the Technical University of Vienna, Vienna, Austria, in 1985 and 1989, respectively. His thesis was "An implant for combined analog and pulsatile electrostimulation of the acoustic nerve."

In 1986 he joined the Institute of Experimental Physics, University of Innsbruck, Austria. His research interests include cochlear implant design, signal processing and RF-power amplifiers.

Erwin S. Hochmair was born in Vienna, Austria, in 1940. He received the Dipl.-Ing. and Dr.techn. degrees in electrical engineering from the Technical University of Vienna, Vienna, Austria, in 1964 and 1967, respectively.

In 1965 he joined the Institute for Physical Electronics, Technical University of Vienna, where he teaches courses on linear integrated circuits and circuit design. From 1970 to 1972 he was with the NASA Marshall Space Flight Center, AL, as a Research Associate. During 1979 he was Visiting Associate Professor at Stanford University, Stanford, CA. Since 1986 he has been a full professor at the Institute of Experimental Physics at the University of Innsbruck, Austria. His current research interests are circuit design, signal processing, and cochlear implant design.